ORIGINAL ARTICLE

Reduced White Matter Fiber Density in Autism Spectrum Disorder

Dennis Dimond[1,2,3,4], Manuela Schuetze[1,2,3], Robert E. Smith[5,6], Thijs Dhollander[5,6], Ivy Cho[7], Sarah Vinette[8], Kayla Ten Eycke[2,9,10,11], Catherine Lebel[2,3,4,11,12,14], Adam McCrimmon[2,11,13], Deborah Dewey[2,9,10,11], Alan Connelly[5,6] and Signe Bray[2,3,4,11,12,14]

[1]Department of Neuroscience, Cumming School of Medicine, University of Calgary, Calgary AB, Canada T2N 4N1, [2]Alberta Children's Hospital Research Institute, University of Calgary, Calgary AB T3B 6A8, Canada, [3]Child and Adolescent Imaging Research Program, University of Calgary, Calgary AB, Canada T3B 6A8, [4]Hotchkiss Brain Institute, University of Calgary, Calgary AB, Canada T2N 4N1, [5]The Florey Institute of Neuroscience and Mental Health, Melbourne VIC 3084, Australia, [6]The Florey Department of Neuroscience and Mental Health, The University of Melbourne, Melbourne VIC 3052, Australia, [7]Department of Psychological Clinical Sciences, University of Toronto, Toronto ON, Canada M5S, [8]Faculty of Medicine, University of Toronto, Toronto ON, Canada M5S, [9]Department of Paediatrics, Cumming School of Medicine, University of Calgary, Calgary AB, Canada T2N 4N1, [10]Department of Community Health Sciences, University of Calgary, Calgary AB, Canada T2N 4N1, [11]Owerko Centre, University of Calgary, Calgary AB, Canada T2N 4N1, [12]Department of Radiology, Cumming School of Medicine, University of Calgary, Calgary AB, Canada T2N 4N1, [13]Werklund School of Education, University of Calgary, Calgary AB, Canada TN2 4N1 and [14]Mathison Centre for Mental Health Research and Education, University of Calgary, Calgary AB, Canada T2N 4N1

Address correspondence to Dennis Dimond. Email: dennis.dimond@ucalgary.ca

Abstract

Differences in brain networks and underlying white matter abnormalities have been suggested to underlie symptoms of autism spectrum disorder (ASD). However, robustly characterizing microstructural white matter differences has been challenging. In the present study, we applied an analytic technique that calculates structural metrics specific to differently-oriented fiber bundles within a voxel, termed "fixels". Fixel-based analyses were used to compare diffusion-weighted magnetic resonance imaging data from 25 individuals with ASD (mean age = 16.8 years) and 27 typically developing age-matched controls (mean age = 16.9 years). Group comparisons of fiber density (FD) and bundle morphology were run on a fixel-wise, tract-wise, and global white matter (GWM) basis. We found that individuals with ASD had reduced FD, suggestive of decreased axonal count, in several major white matter tracts, including the corpus callosum (CC), bilateral inferior frontal-occipital fasciculus, right arcuate fasciculus, and right uncinate fasciculus, as well as a GWM reduction. Secondary analyses assessed associations with social impairment in participants with ASD, and showed that lower FD in the splenium

of the CC was associated with greater social impairment. Our findings suggest that reduced FD could be the primary microstructural white matter abnormality in ASD.

Key words: autism spectrum disorder, fiber density, fixel-based analysis, social impairment, white matter

Introduction

Autism spectrum disorder (ASD) is a neurodevelopmental disorder characterized by difficulties in social interactions and communication, and restricted interests and repetitive behaviors (American Psychiatric Association 2013). Studies in typically developing (TD) and clinical populations have associated social skills with structural properties of white matter tracts, including the uncinate fasciculus (UF), arcuate fasciculus (AF), inferior longitudinal fasciculus (ILF), and superior longitudinal fasciculus (SLF) (Kumar et al. 2010; Cheon et al. 2011; Poustka et al. 2012; Im et al. 2018). It has therefore been hypothesized that structural alterations in these tracts may be related to social impairment in ASD.

Supporting this hypothesis, studies using diffusion tensor imaging (DTI) tractography and voxel-based analyses (VBA) in ASD have shown decreased fractional anisotropy (FA) and increased mean diffusivity (MD) in tracts related to social processing (Aoki et al. 2013; Ameis and Catani 2015; Di et al. 2018). Abnormalities are frequently reported in the UF, AF, cingulum, corpus callosum (CC), ILF, SLF, and inferior fronto-occipital fasciculus (IFOF) (for reviews see Ameis and Catani 2015 and Travers et al. 2012). DTI metrics are sensitive to various microstructural characteristics however, therefore the specific pathology underlying these findings is unknown. A recent postmortem (Zikopoulos and Barbas 2010) study suggests that axonal density may be reduced in ASD, which could explain commonly reported FA decreases.

DTI findings are not always consistent however; a recent meta-analysis showed that there is high variability across studies, in terms of both the location and direction of group differences (Ameis and Catani 2015). While this variability may reflect heterogeneity among individuals with ASD, it may also be due in part to methodological challenges associated with DTI. Specifically, the inability to resolve multiple fiber orientations in regions of crossing/kissing fiber geometry may contribute to unreliable estimates of FA and MD in these regions (Jeurissen et al. 2013). Higher-order diffusion models and tract-specific metrics with greater structural-specificity may help to resolve some of the ambiguity surrounding white matter abnormalities in ASD and how they relate to social impairments.

Fixel-based analysis (FBA; Raffelt, Tournier et al. 2017), a recently developed analytic framework that facilitates measurement and statistical analysis of micro- and macrostructural metrics within "fixels" (specific fiber-bundle populations within a voxel (Raffelt et al. 2015) could be used to resolve some of the inconsistencies in the research literature. FBA typically utilizes the fiber orientation distributions (FODs) estimated using constrained spherical-deconvolution (CSD) techniques (Tournier et al. 2007), that are capable of resolving multiple fiber-bundle populations within a voxel, thereby making it possible to calculate metrics that are tract specific. These metrics include fixel-wise fiber density (FD), fiber cross-section (FC), and a combined metric, fiber density and cross-section (FDC), which are arguably of greater structural-specificity and more easily interpretable than traditional voxel-wise DTI metrics (Raffelt, Tournier et al. 2017). FBA could therefore provide novel insight into white matter abnormalities in ASD and how they relate to social impairment.

The aim of this study was to utilize FBA to assess fixel-specific white matter measures in ASD and to determine if these white matter properties are associated with social impairment. Considering postmortem findings of reduced axonal density (Zikopoulos and Barbas 2010), and DTI findings of reduced FA in tracts related to social processing in ASD (Aoki et al. 2013; Ameis and Catani 2015; Di et al. 2018), we hypothesized that relative to healthy controls, participants with ASD would have reduced FD in white matter fiber bundles that have been previously implicated in social function. We further hypothesized that reduced FD in these fiber bundles would correlate with social impairment in participants with ASD. In order to compare FBA results with commonly used DTI metrics, we also conducted VBA to look at group differences in FA and MD, and associations between these metrics and social impairment.

Table 1. Group comparison of participant characteristics: SD = Standard deviation; ICV = Intra-cranial volume; SRS-2 = Social Responsiveness Scale—second edition; PRI = Perceptual Reasoning Index; ∗ indicates significant group difference in independent sample t-test ($P < 0.05$)

	ASD ($n = 25$)		TD ($n = 27$)				
	Mean	SD	Mean	SD	T-statistic	Chi-square	P-value
Sex (M:F)	21:4		21:6		–	0.324	0.569
Handedness (R:L)	22:3		25:2		–	0.315	0.575
Age (years)	16.8	2.26	16.9	2.07	−0.13	–	0.901
ICV (cm^3)	1547.2	152.4	1567.3	148.3	−0.48	–	0.632
SRS-2	75.8	8.56	43.6	4.61	17.1	–	<0.001*
FSIQ	91.6	17.0	109	11.9	−4.47	–	<0.001*
VIQ	85.9	16.3	109	11.4	−5.92	–	<0.001*
PRI	99.8	17.0	109	13.3	−2.19	–	0.034*

Materials and Methods

Participants

We collected MRI data from 27 participants with ASD and 31 TD participants between the ages of 14 and 20 years (Table 1), who participated in a larger study (Cho et al. 2017). Exclusion criteria were contraindications to MRI and a history of neurological or psychiatric symptoms for the TD participants, though one TD participant was included who self-reported dyslexia. Seven participants with ASD reported one or more co-occurring diagnoses, and 6 participants with ASD were taking one or more psychoactive medication at the time of data collection (see Supplementary Table S1). All participants with ASD were administered the autism diagnostic observation schedule, second edition (ADOS-2; Lord et al. 2012) by a research reliable rater, and scored at or above the cut-off for ASD. Due to technical issues, we did not acquire diffusion-weighted images (DWI) for one participant with ASD and for one TD participant. We excluded one participant with ASD due to data quality and 3 TD participants due to missing IQ and handedness data (described in more detail below). The final sizes of the ASD and TD groups were therefore 25 participants with ASD and 27 TD participants. Written informed consent was obtained from all participants over the age of 18 years and assent with parental consent was obtained from participants younger than 18. The study procedures were approved by the University of Calgary Conjoint Health Research Ethics Board.

Cognitive and Neuropsychological Assessments

Social functioning was assessed using the Social Responsiveness Scale, Second Edition (SRS-2; Constantino 2012), which is a valid measure to assess social impairment in children with and without ASD. For our analyses, we used the age-standardized SRS-2 Total T-Score (subsequently referred to simply as "SRS-2 scores") as an index of social impairment, with higher scores indicating greater social deficit. Participants were asked about their handedness and completed an IQ assessment. These were used as covariates in our models. To assess IQ, we utilized the Wechsler Abbreviated Scale of Intelligence, Second Edition (WASI-II; Wechsler 2011), which provides measures for verbal, perceptual, and full-scale IQ. To control for group differences in IQ in statistical analyses, we utilized the Perceptual Reasoning Index (PRI) subscale of the WASI-II. The PRI assesses non-verbal fluid abilities, which have been suggested to capture intellectual functioning in individuals with ASD more accurately, as compared with measures that demand verbal skills (Qiu et al. 2010).

MRI Data Acquisition

MRI data were acquired on a 3 T GE MR750w (Waukesha, WI) scanner at the Alberta Children's Hospital using a 32-channel head coil. MRI data included DWIs and a structural T1-weighted image, both acquired while participants watched a video of their choice. DWIs were acquired via a 2D spin echo EPI sequence (b = 2000 s/mm^2, 30 diffusion-weighted directions, 5 interspersed b0 images, 2.2 mm isotropic voxels, 50 slices, 22 × 22 cm FOV, TE = 88.0 ms, TR = 12000 ms). A 3D BRAVO sequence (flip angle: 10°, 24 × 24 cm FOV, TI = 600, 0.8 mm isotropic voxels) was used to acquire structural images.

Structural Image Processing

Structural T1-weighted images were utilized in DWI EPI-susceptibility distortion correction, and to calculate intra-cranial volume (ICV) for use as a nuisance covariate in statistical analysis. It is generally recommended to include ICV as a covariate in FBAs of structural metrics to account for relative differences in head size, which may vary between groups and can potentially influence structurally related fixel-based white matter metrics. T1-weighted images were bias field corrected (Tustison et al. 2010) prior to use. To calculate ICV, we first segmented the structural image into white matter, gray matter, and cerebrospinal fluid components in SPM12 (https://www.fil.ion.ucl.ac.uk/spm/software/spm12/; last accessed January 4, 2019). The values in these images were then summed and the resulting value was multiplied by the image voxel size (0.8 × 0.8 × 0.8 mm) to get ICV in cm^3.

DWI Pre-processing

To mitigate effects of head motion, we utilized recently-released updates to state-of-the-art DWI pre-processing (Andersson and Sotiropoulos 2016) provided in FSL (https://fsl.fmrib.ox.ac.uk/fsl/fslwiki/; last accessed January 4, 2019), including replacement of slice-wise signal dropout (Andersson et al. 2016) and within-volume motion correction (Andersson et al. 2017). Diffusion-weighted volumes for which more than 10% of slices were classified as containing signal dropout were removed from the data, and subjects for whom more than 10% of volumes were removed were excluded from the study (resulting in exclusion of one participant with ASD). Following initial pre-processing, we performed bias field correction (Tustison et al. 2010) and upsampled DWI data to 1.25 mm isotropic. We then calculated FODs for each participant via single-shell 3-tissue constrained spherical-deconvolution (SS3T-CSD) using a group averaged response function for each tissue type (gray matter, white matter, and CSF) (Raffelt, Tournier, Rose, et al. 2012; Dhollander et al. 2016; Dhollander and Connelly 2016a). We then performed global intensity normalization on subjects' FOD images to make FOD amplitudes comparable across participants (Raffelt, Dhollander et al. 2017). Lastly, we performed EPI-susceptibility distortion correction via non-linear registration (constrained to the phase-encoding direction) of participants' DWIs and T1-weighted structural images, guided by a pseudo-T1-weighted contrast estimated from SS3T-CSD (Dhollander and Connelly 2016a, 2016b). Except for initial motion pre-processing performed in FSL, all subsequent pre-processing and analysis steps were conducted in MRtrix3 (www.mrtrix.org; last accessed January 4, 2019). A schematic of the methodological approach utilized in this study is provided in Figure 1.

Fixel Metrics

Processing steps for FBA included: generating a study specific FOD template (Raffelt et al. 2011); registration of subject FODs into template space to achieve spatial correspondence (Raffelt, Tournier, Crozier, et al. 2012); segmentation of both the subject's warped FODs and the FOD template image to identify the number and orientation of fixels in each voxel (Smith et al. 2013); and finally, identification of fixel correspondence between subjects and the template, such that template fixels have subject-wise fixel metrics assigned to them.
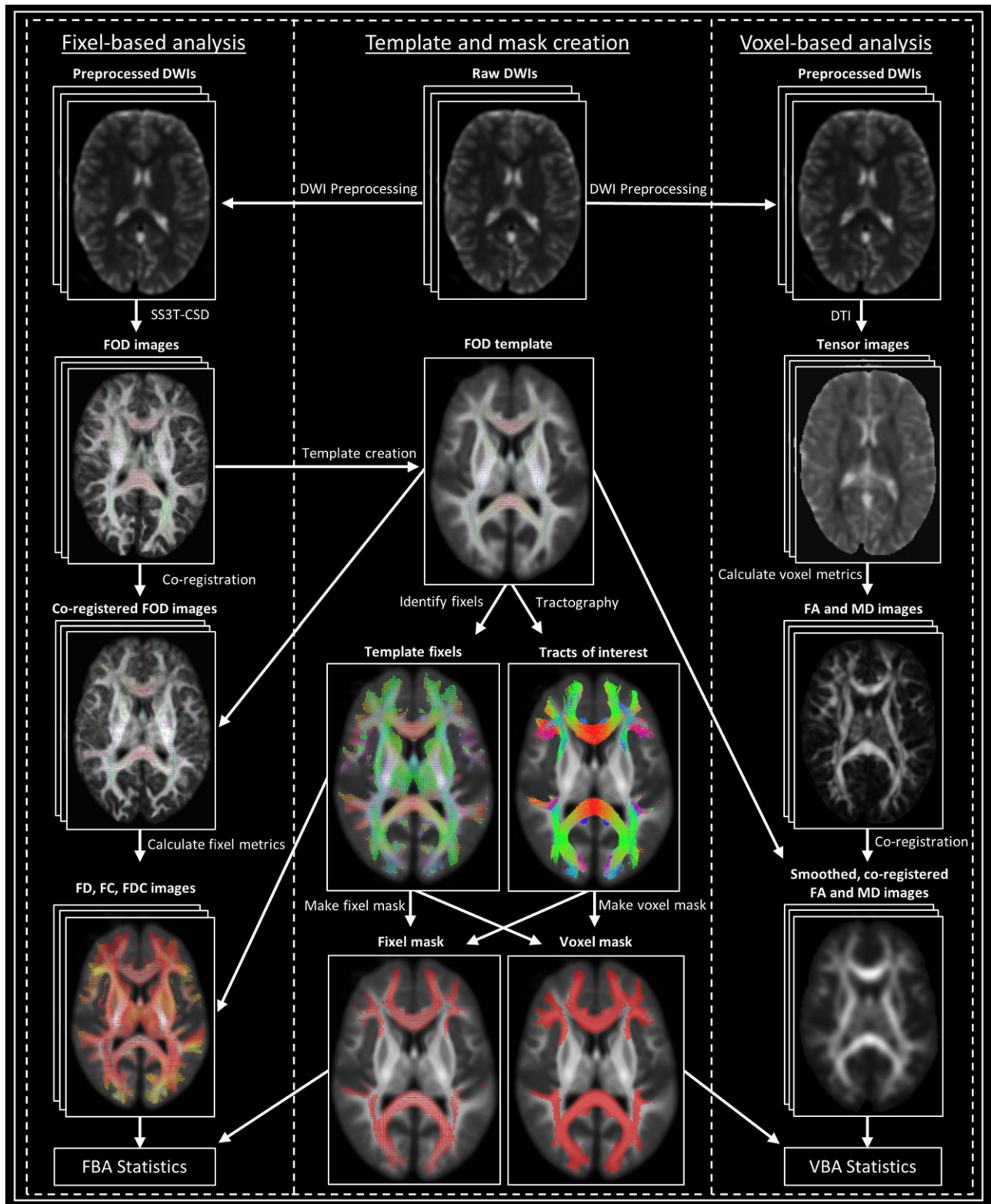
Figure 1. Methods schematic. Visual overview of the processing steps involved in the fixel- and voxel-based analyses utilized in the study. Processing steps specific to the fixel-based analysis are shown on the left panel, while those specific to the voxel-based analysis are shown on the right panel. The center panel depicts steps involved in both analyses. DWIs = diffusion-weighted images; FOD = fiber orientation distribution; FA = fractional anisotropy; MD = mean diffusivity; FD = fiber density; FC = fiber cross-section; FDC = fiber density and cross-section; FBA = fixel-based analysis; VBA = voxel-based analysis.

Within this pipeline, 3 fixel-based metrics were calculated for analysis:

- *Fiber density (FD)*, or apparent fiber density (Raffelt, Tournier, Rose, et al. 2012), is a metric related to the restricted intra-axonal diffusion compartment. FD is calculated as the integral of a given fixel's FOD and is proportional to the intra-axonal volume of fiber bundles aligned with that fixel (Raffelt, Tournier, Rose, et al. 2012).
- *Fiber cross-section (FC)*, is a relative measure of individual differences in fiber-bundle diameter, and is calculated as the extent of distortion perpendicular to a given fixel's orientation that is required to warp a subject's FOD image into template space (Raffelt, Tournier et al. 2017).
- *Fiber density and cross-section (FDC)*, is the product of FD and FC, which is computed to assess combined changes to both micro- and macro-structures.

For an in-depth description of the FBA pipeline and associated metrics, see (Raffelt, Tournier et al. 2017).

Voxel Metrics

To compare results from fixel-based metrics to more commonly reported voxel-wise metrics such as FA and MD, we additionally conducted a VBA. Following DWI pre-processing as described above, we utilized the diffusion tensor model to calculate FA and MD maps for each subject. These maps were then warped into the same study template space utilized in the FBA. Maps were smoothed using a 5.5 mm FWHM Gaussian smoothing kernel.

Template-based Tractography and Analysis Masks

A whole-brain tractogram was generated both for use in FBA statistical enhancement, and to define analysis masks for our FBA and VBA. This tractogram was generated via probabilistic tractography upon the FOD template, seeding randomly within the brain until 20 million streamlines were delineated (tractography parameters: step size = 0.625 mm, max angle between steps = 22.5°, min/max fiber length = 10 mm/250 mm, cut-off FOD amplitude = 0.1). The tractogram was then reduced to 2 million streamlines via the spherical-deconvolution informed filtering of tractograms (SIFT) algorithm (Smith et al. 2013).

To improve statistical power, we limited our analysis to major white matter bundles in which abnormalities have been previously reported in ASD (Travers et al. 2012; Ameis and Catani 2015); these included the cingulum, AF, SLF, ILF, IFOF, and UF bilaterally, as well as the CC. Using manually-defined inclusion and exclusion ROIs, we extracted these fiber bundles individually from the template tractogram (see Supplementary Table S2 for details). The streamlines corresponding to these bundles of interest were then concatenated together and used to generate a fixel analysis mask that included only those fixels through which at least 5 streamlines passed and that had an FOD amplitude of at least 0.1. This fixel mask was subsequently used to define a voxel mask that included only those voxels containing at least one fixel in the fixel mask. The resulting FBA and VBA masks are shown in Figure 2A–B, while the tracts utilized in creating these masks are shown in Figure 2C.

In addition to FBAs and VBAs, we also performed tract-wise and global white matter (GWM) averaged analyses of the quantitative measures of interest. For each tract of interest, we generated individual fixel and voxel masks from the delineated streamlines bundles using the same criteria as described above; within each tract of interest, the mean value of the measure of interest (i.e. FD, FC, FDC, FA, MD) for each subject was then calculated. Finally, the mean value of each parameter of interest throughout all fixels and corresponding voxels in the brain that had an FOD amplitude of 0.1 or above was additionally calculated for each subject as a GWM summary measure.

Head-motion Assessment

Head motion during DWI acquisition is prevalent in individuals with ASD and can confound group comparisons of white matter properties (Koldewyn et al. 2014; Yendiki et al. 2014; Solders et al. 2017). To quantify and control for potential residual influence of head motion on statistical analyses, we calculated several motion metrics to be compared across groups and used as covariates in statistical analyses, if group differences were present. These metrics were calculated from output of FSL pre-processing steps, and included: (1) excluded volumes, the total number of volumes that were removed due to motion–corruption; (2) total dropout slices, the total number of slices across all volumes classified as containing signal dropout; (3) average dropout slices, the average number of dropout slices per volume in volumes that contained at least one dropout slice; (4) mean translation (in mm) and (5) mean rotation (in degrees), calculated as the average of the translational and rotational registration parameters in registering each DWI slice to the b0 image; and (6) frame-wise displacement, calculated as the average of all registration parameters, after converting the rotational parameters from degrees to millimeters about a 50-mm sphere (Power et al. 2012). These metrics were compared between groups in SPSS 24 (Corp. 2016). All except total dropout slices were non-parametrically distributed; therefore, Mann–Whitney *U*-tests were utilized to compare these metrics. Total dropout slices was the only motion metric that was significantly different between groups (Supplementary Table S3); it was therefore included as a nuisance covariate in group comparisons of white matter metrics.

Statistical Analysis

Independent-sample *t*-tests were utilized to compare age, ICV, full-scale IQ, verbal IQ, PRI, and SRS-2 scores between groups, while Chi-square tests were utilized to compare handedness and sex. These tests were conducted in SPSS 24 (Corp. 2016).

For FBA and VBAs, general linear models (GLM) were utilized to compare fixel-wise FD, FC, and FDC, as well as voxel-wise FA and MD between groups, controlling for age, sex, handedness, ICV, total dropout slices, and PRI. GLM regressions were utilized to assess associations between white matter metrics and SRS-2 scores in participants with ASD. For FBAs, connectivity-based smoothing and statistical inference were conducted using the connectivity-based fixel enhancement (CFE) method (Raffelt et al. 2015), which performs permutation-based statistical inference of fixel-wise quantitative measures in the presence of crossing fibers. For VBAs, statistical inference was also performed using non-parametric permutation testing, but using the threshold-free cluster enhancement (TFCE) method (Smith and Nichols 2009). In both analyses, we used family-wise error (FWE) correction for multiple comparisons, with statistical significance at $P < 0.05$.

To compare tract-wise mean FD, FC, FDC, FA, and MD across groups, as well as the GWM averaged measures, we conducted a series of ANCOVAs in SPSS 24 (Corp. 2016), while controlling for
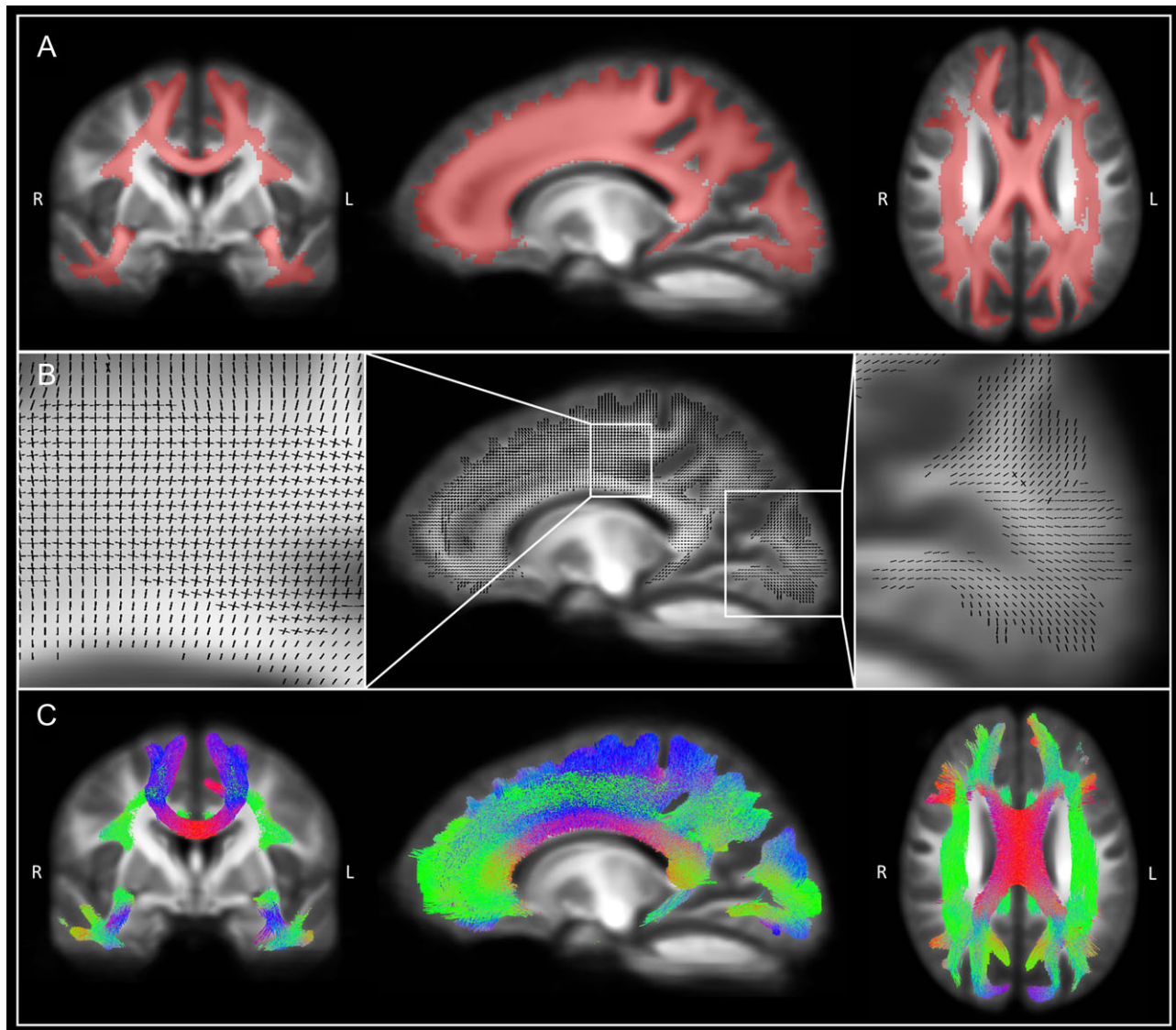
Figure 2. Analysis masks and tracts. (A) Voxel analysis mask visualized as a red overlay on 2D slices of the study template FOD image. (B) Fixel analysis mask overlaid onto a 2D sagittal slice of the study template FOD image (center), with fixels depicted as black lines. Windows to the left and right show zoomed in images of the regions enclosed in white squares within the central window. (C) Tracts that were utilized in defining the analysis masks (cingulum, AF, SLF, ILF, IFOF, UF, and corpus callosum), visualized as 3D streamlines within 2D slices of the study template FOD image. Streamlines are colored by direction: red = left–right; green = anterior–posterior; blue = superior–inferior.

age, sex, handedness, ICV, total dropout slices, and PRI. To look for associations between tract-wise means and SRS-2 scores in participants with ASD, we conducted a series of Spearman correlations. Here, we used false discovery rate (FDR) to correct for multiple comparisons, with statistical significance set at $q < 0.05$. FDR was utilized to correct for 14 comparisons (6 bilateral tracts + the CC and GWM measure) within each metric.

Finally, to account for potential influence of comorbidities and psychoactive medication, we conducted all aforementioned analyses again with a subsample of participants, in which we excluded participants with ASD who had a diagnosed comorbidity, or who were suspected of having an undiagnosed comorbidity based on a prescribed psychoactive medication. Based on these criteria, 9 participants with ASD were excluded from the subsample, leaving 16 participants with ASD, and 27 TD participants (see Supplementary Table S4 for details).

Results

Demographics

The 2 groups were not significantly different in terms of sex, handedness, age, or ICV, though participants with ASD had higher SRS-2 scores, and lower PRI scores relative to TD participants (Table 1).

Group Comparisons

FBA showed that participants with ASD had decreased FD relative to the TD participants in several fixels within the CC, as well as in the IFOF bilaterally (Fig. 3A). In the CC, reduced FD was found in a segment of the splenium in the right hemisphere and within branches extending into the frontal cortex bilaterally. Within the IFOF, significantly reduced FD was found in fixels
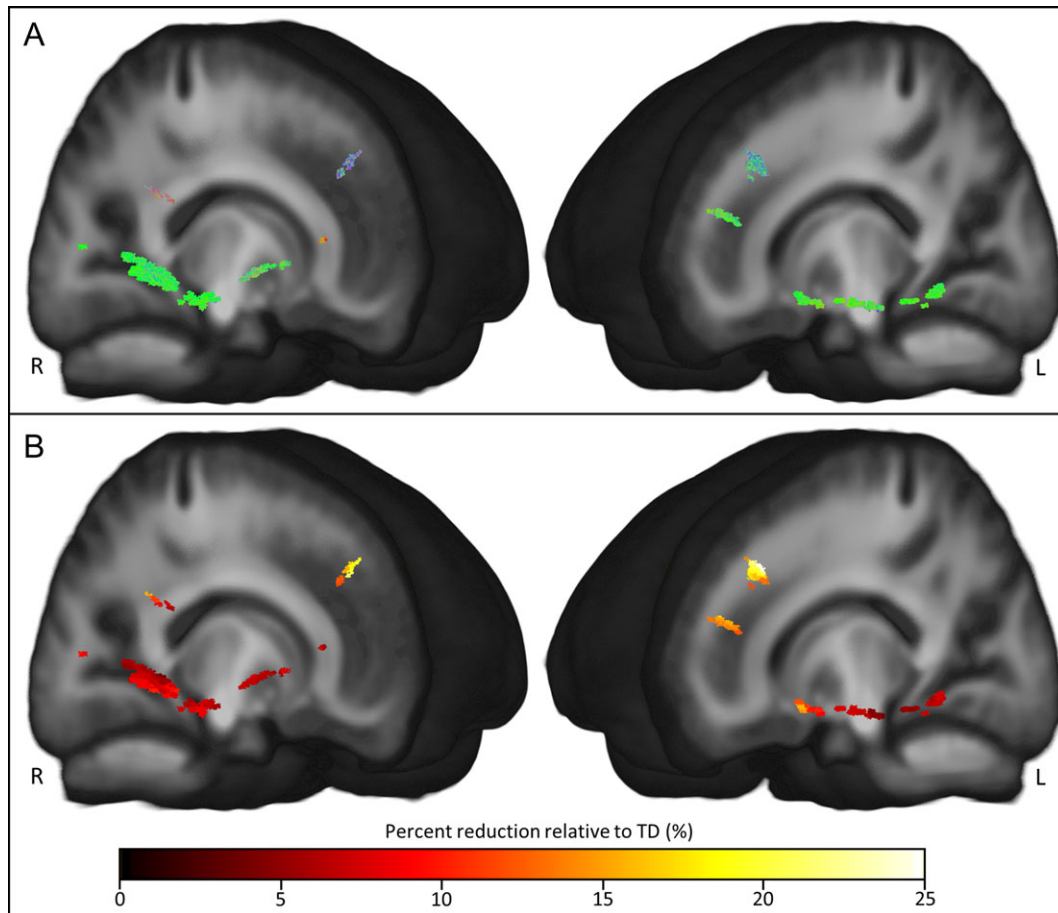
Figure 3. Reduced fixel-wise fiber density in participants with ASD compared with typical controls. Fixels in which fiber density was reduced in participants with ASD relative to controls, visualized as 3D fixels overlaid onto a 3D brain image of the study template FOD. (A) Fixels are colored by direction: red = left–right; green = anterior–posterior; blue = superior–inferior. (B) Fixels are colored by percent reduction in fiber density relative to the typically developing (TD) controls.

along the full length of the tracts bilaterally, with a more spatially-extensive difference in the right hemisphere. Percent reductions in FD were greatest for fixels in the frontal branches of the CC (Fig. 3B). We found no group differences in fixel-wise FC or FDC. VBA showed no group differences in FA or MD.

Consistent with the hypothesis driven approach to this study, fixel- and voxel-based analyses were restricted to white matter regions believed to house abnormalities in ASD. However, considering this approach might miss group differences in regions outside of our analysis mask, we conducted follow-up analyses in which we compared structural metrics between groups at every fixel/voxel in the brain. Results of these follow-up analyses revealed similar findings to those seen with our spatially restricted mask; FD was reduced in the right IFOF and in segments of the CC, and there were no group differences in FC, FDC, FA, or MD.

Similar to the FBA results, in our tract-wise analysis we found reduced FD in the CC, though reductions in the left and right IFOF fell below significance (uncorrected $P = 0.027$, $q = 0.054$ and uncorrected $P = 0.031$, $q = 0.054$, respectively). We also found significantly reduced FD in the right AF and right UF, as well as trendline reductions in the left UF (uncorrected $P = 0.028$, $q = 0.054$) and right SLF (uncorrected $P = 0.043$, $q = 0.0758$). GWM-FD was also reduced in participants with ASD. This global reduction, alongside significant and trendline reductions in several major white matter tracts, suggests

reduced FD may be a GWM property in participants with ASD. These reductions all had a moderate effect size, though the effect was strongest in the right UF, and weakest in the GWM (Fig. 4; Supplementary Table S5). There were no significant differences in tract-wise or GWM-FC, FDC, FA, or MD.

Social Impairment Correlations

In the participants with ASD, a negative association was found between SRS-2 scores and FD of fixels within the splenium of the CC, extending through the optic radiata towards the occipital lobe (Fig. 5). No significant associations were found between SRS-2 scores and fixel/voxel-wise FC, FDC, FA, or MD. In tract-wise and GWM analyses, no significant associations were found between SRS-2 scores and GWM or tract-wise FD, FC, FDC, FA, or MD.

Analyses in Participants Without Comorbidities or Medications

To ensure our results were not confounded by effects of comorbidities and psychoactive medication, we conducted statistical analyses with a subsample of participants, excluding those with comorbidities, or prescribed psychoactive medication.

Similar to findings with the full study sample, in our FBA we found that participants with ASD had reduced FD in the IFOF

bilaterally, as well as in the genu of the CC (Supplementary Fig. S1). No group differences were found with any of the other fixel- or voxel-wise metrics.

Group comparison of tract-means also revealed similar findings to those found in the full study sample. We found that mean FD was reduced in the right AF, right UF, L-IFOF, and in the CC, with trendline reductions in GWM-FD (Supplementary Table S6). There were no significant differences in tract-wise or GWM-FC, FDC, FA, or MD.

Finally, we tested for an association between SRS-2 scores and white matter metrics at the fixel-, voxel-, and tract-wise basis, however no significant associations were found in our subsample of participants with ASD.
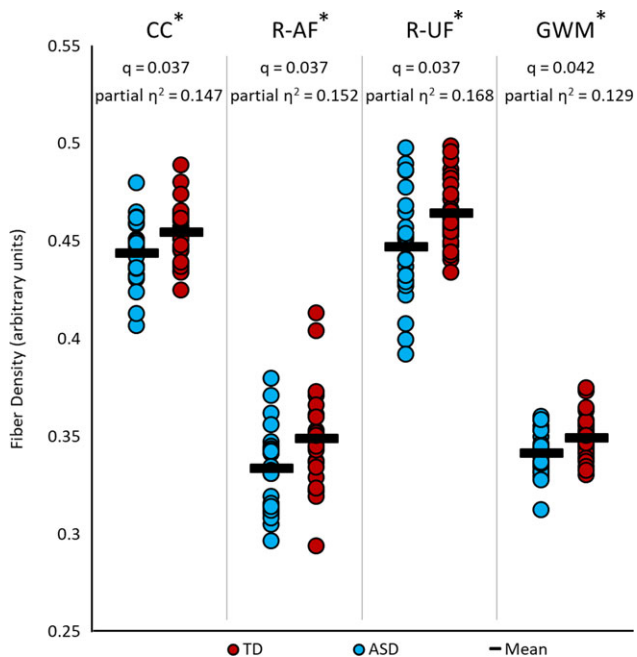

Figure 4. Reduced tract mean fiber density in participants with ASD compared with typical controls. Individual participant mean FD values for tracts in which average FD was reduced in individuals with ASD relative to controls. ∗ indicates tracts that were significantly different after FDR correction ($q < 0.05$). CC = corpus callosum; R-AF = right arcuate fasciculus; R-UF = right uncinate fasciculus; GWM = global white matter.

Discussion

In this study, we sought to determine if there were tract-specific differences in white matter FD, FC, and FDC between individuals with ASD and TD controls, and whether these properties were related to social impairment in individuals with ASD. We found reduced FD of fixels in the splenium and genu of the CC, and IFOF bilaterally in individuals with ASD. We also found that mean FD was reduced in the CC, right AF, right UF, and in white matter as a whole. In participants with ASD, reduced FD of fixels in the splenium of the CC was associated with greater social impairment. Notably, we found no group differences in, or social impairment associations with, FA or MD. To the best of our knowledge, this is the first application of FBA to investigating white matter abnormalities in ASD. Our findings provide evidence that reduced FD may be the primary microstructural white matter abnormality in individuals with ASD.

Our findings of reduced FD in the CC and IFOF at the fixel level, as well as reductions in mean FD of the CC, right AF and right UF in ASD suggest that there is decreased intra-axonal volume of specific white matter tracts, potentially reflecting a reduction in the number of axons. Reduced axonal density in ASD has been previously suggested by both diffusion imaging (Lazar et al. 2014) and postmortem (Zikopoulos and Barbas 2010) studies, reporting decreased axonal water fraction (a measure comparable to the FD metric used here), and fewer large-caliber axons in individuals with ASD, respectively. Previous DTI studies have also found evidence for microstructural abnormalities in the CC (Cheon et al. 2011; Poustka et al. 2012; Aoki et al. 2013; Di et al. 2018), IFOF (McGrath et al. 2013; Im et al. 2018), UF (Cheon et al. 2011; Poustka et al. 2012; Chang et al. 2014), and AF (Kumar et al. 2010; Aoki et al. 2013), which is broadly neuroanatomically consistent with our findings. However, findings from DTI can be challenging to interpret as metrics are quantified at the voxel level and therefore cannot be easily attributed to specific fiber-bundles, such as those traversed by the IFOF (Jeurissen et al. 2013). Our fixel-wise results help to consolidate DWI evidence of microstructural abnormalities in these tracts by demonstrating fiber-bundle specific differences in crossing fiber regions in ASD.

In addition to tract-specific reductions in FD, we also found that GWM-FD was reduced in participants with ASD, though to a lesser extent as compared to that of reductions in specific fiber bundles. This suggests that while reductions in axonal count may be more prominent in specific white matter fiber bundles, this may be a global property of white matter tracts in
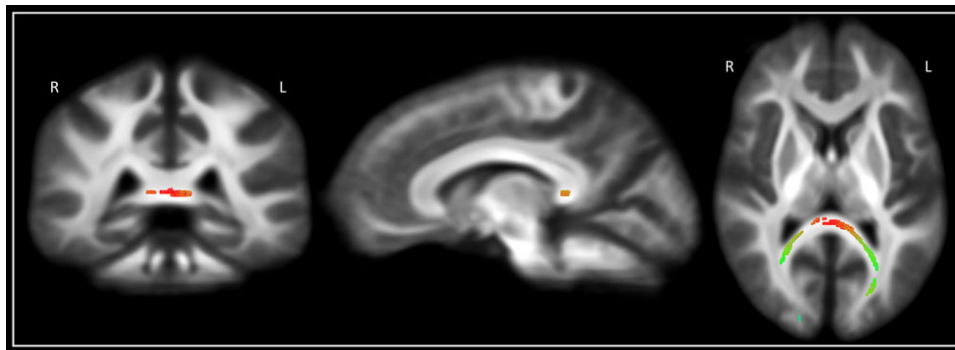

Figure 5. Negative correlation between fixel-wise fiber density and social impairment in participants with ASD. Fixels in which fiber density correlated negatively with SRS-2 scores in participants with ASD, visualized as 3D fixels overlaid onto a 2D slice of the study template FOD image. Fixels are colored by direction: red = left–right; green = anterior–posterior; blue = superior–inferior.

ASD. Interpretation of these findings as evidence of a global reduction, rather than being driven by reductions in select tracts, is supported by our finding of trendline reductions in several white matter fiber bundles, and in considering that the global metric was calculated across ~8 times as many fixels as in the FBA mask. The notion of a global reduction in white matter microstructure in ASD is consistent with DTI evidence of widespread FA reductions and MD increases in ASD participants (Travers et al. 2012; Ameis and Catani 2015). Interestingly however, we found no group differences in voxel- or tract-wise FA or MD in the current study. There are multiple possible reasons for this. For example, results of DTI studies in ASD are known to be influenced by cohort age (Duerden et al. 2012) and head-motion confounds (Koldewyn et al. 2014; Yendiki et al. 2014; Solders et al. 2017; Boets et al. 2018). Our diffusion-weighted imaging data was also acquired at a higher b-value than is commonly used in DTI studies, which may have been a factor. Regardless, the fact that we found differences in FD but not FA or MD suggests that FBA metrics may be more sensitive to the white matter abnormalities present in ASD.

In addition to applying FBA to detect white matter abnormalities in ASD, we also sought to determine if these abnormalities had a linear relationship with social impairment. We found that reduced FD of the splenium of the CC in individuals with ASD was associated with greater social impairment. CC abnormalities are one of the more consistently reported white matter findings in ASD (Travers et al. 2012), as are abnormalities in the uncinate and arcuate fasciculi (Ameis and Catani 2015), which were also found to have reduced FD in our study. Numerous diffusion imaging studies have linked behavioral symptoms to white matter abnormalities in ASD (Cheon et al. 2011; Poustka et al. 2012; McGrath et al. 2013; Im et al. 2018), some of which have found associations in regions that co-localize with our findings. Abnormalities in the CC, IFOF, and UF have been related to deficits in social skills (Alexander et al., 2007; Gibbard et al., 2013), visuospatial skills and processing speed (McGrath et al. 2013), and communication and interaction difficulties (Poustka et al. 2012), respectively. It is possible that beyond the relationship between splenium FD and social impairment reported here, reduced FD in the CC, IFOF, and UF may be related to deficits in these cognitive and behavioral functions, which have been implicated in ASD.

Strengths of the current study include the use of FBA to investigate tract-specific white matter abnormalities, as well as a thorough assessment of head motion and application of both correction and regression to mitigate potential confounding effects. This study does however have several limitations. First, diffusion data were collected for a single non-zero b-value only (so called "single-shell" data), with a relatively low-angular resolution (30 directions) and limited diffusion-weighting ($b = 2000\,\text{s/mm}^2$) compared with what is typically recommended for the CSD model (Tournier et al. 2013) and quantification of apparent FD (Raffelt, Tournier, Rose, et al. 2012). To mitigate this, we utilized the state-of-the-art Single-Shell 3-Tisssue CSD (SS3T-CSD) method (Dhollander and Connelly 2016a) that additionally takes into account the presence of other tissue types such as gray matter-like tissues (Dhollander et al. 2017), which would otherwise still have a significant contribution to the diffusion signal at this level of diffusion-weighting. Second, as part of our pre-processing pipeline, we removed DWI volumes that were deemed to be severely corrupted by motion. While the impact of omitting DWI volumes on FBA metrics is unknown, discarding DWI volumes has been shown to influence FA, with increasingly detrimental effects with more

rejected volumes (Chen et al. 2015). However, considering volumes were only rejected for a handful of subjects (~15%), with no more than 3 volumes rejected per subject, and there was no significant difference between groups in the number of volumes excluded, such volume rejection is unlikely to have greatly influence our results. Third, our study sample included participants with comorbidities and participants who were taking psychoactive medications at the time of data collection. To examine the potential influence of these factors, we conducted analyses with and without these participants included. Excluding these participants did not influence the results of our group comparisons, however the association between social deficits and splenium FD did not reach statistical significance in our subsample of participants with ASD. While we suspect this was the result of decreased statistical power rather than confounding effects of comorbid diagnoses and medication, future studies will be necessary to resolve these findings.

In sum, the aim of this study was to utilize FBA to assess white matter FD and cross-section FC in ASD and to determine if these white matter properties are related to severity of social impairment. Here, we report reductions in FD, suggestive of decreased axonal count, in white matter as a whole and within specific white matter fiber bundles, including the CC where reduced FD of the splenium was associated with greater social impairment in individuals with ASD. This suggests that FD may be a sensitive marker for atypical white matter in ASD. Collectively, our results provide novel insight into the biological underpinnings of white matter abnormalities in ASD and their relationship with core disorder symptoms, suggesting decreased axonal count may be the primary white matter abnormality.

Supplementary Material

Supplementary material is available at *Cerebral Cortex* online.

Funding

Notes

References

Alexander AL, Lee JE, Lazar M, Boudos R, DuBray MB, Oakes TR, Miller JN, Lu J, Jeong EK, McMahon WM, et al. 2007. Diffusion tensor imaging of the corpus callosum in Autism. Neuroimage. 34:61–73.

Ameis SH, Catani M. 2015. Altered white matter connectivity as a neural substrate for social impairment in Autism Spectrum Disorder. Cortex. 62:158–181.

American Psychiatric Association. 2013. Diagnostic and Statistical Manual of Mental Disorders. Washington, DC: American Psychiatric Association.

Andersson JLR, Graham MS, Drobnjak I, Zhang H, Filippini N, Bastiani M. 2017. Towards a comprehensive framework for movement and distortion correction of diffusion MR images: Within volume movement. Neuroimage. 152:450–466.

Andersson JL, Graham MS, Zsoldos E, Sotiropoulos SN. 2016. Incorporating outlier detection and replacement into a non-parametric framework for movement and distortion correction of diffusion MR images. Neuroimage. 141:556–572.

Andersson JLR, Sotiropoulos SN. 2016. An integrated approach to correction for off-resonance effects and subject movement in diffusion MR imaging. Neuroimage. 125:1063–1078.

Aoki Y, Abe O, Nippashi Y, Yamasue H. 2013. Comparison of white matter integrity between autism spectrum disorder subjects and typically developing individuals: a meta-analysis of diffusion tensor imaging tractography studies. Mol Autism. 4:25.

Boets B, Van Eylen L, Sitek K, Moors P, Noens I, Steyaert J, Sunaert S, Wagemans J. 2018. Alterations in the inferior longitudinal fasciculus in autism and associations with visual processing: a diffusion-weighted MRI study. Mol Autism. 9: 10.

Chang YS, Owen JP, Desai SS, Hill SS, Arnett AB, Harris J, Marco EJ, Mukherjee P. 2014. Autism and sensory processing disorders: shared white matter disruption in sensory pathways but divergent connectivity in social-emotional pathways. PLoS One. 9:e103038.

Chen Y, Tymofiyeva O, Hess CP, Xu D. 2015. Effects of rejecting diffusion directions on tensor-derived parameters. Neuroimage. 109:160–170.

Cheon KA, Kim YS, Oh SH, Park SY, Yoon HW, Herrington J, Nair A, Koh YJ, Jang DP, Kim YB, et al. 2011. Involvement of the anterior thalamic radiation in boys with high functioning autism spectrum disorders: a Diffusion Tensor Imaging study. Brain Res. 1417:77–86.

Cho IYK, Jelinkova K, Schuetze M, Vinette SA, Rahman S, McCrimmon A, Dewey D, Bray S. 2017. Circumscribed interests in adolescents with Autism Spectrum Disorder: a look beyond trains, planes, and clocks. PLoS One. 12:e0187414.

Constantino J. 2012. Social Responsiveness Scale, Second Edition (SRS-2). Torrance, CA: Western Psychological Services.

Dhollander T, Connelly A. 2016a. A novel iterative approach to reap the benefits of multi-tissue CSD from just single-shell (+b = 0) diffusion MRI data. In: Singapore: 24th International Society of Magnetic Resonance in Medicine. 3010.

Dhollander T, Connelly A. 2016b. Generating a T1-like contrast using 3-tissue constrained spherical deconvolution results from single-shell (or multi-shell) diffusion MR data. In: ISMRM Workshop on Breaking the Barriers of Diffusion MRI. Lisbon, Portugal. p. 6.

Dhollander T, Raffelt D, Connelly A. 2016. Unsupervised 3-tissue response function estimation from single-shell or multi-shell diffusion MR data without a co-registered T1 image. In: Lisbon, Portugal: Proceedings of ISMRM Workshop on Breaking the Barriers of Diffusion MRI. 5.

Dhollander T, Raffelt D, Connelly A. 2017. Towards interpretation of 3-tissue constrained spherical deconvolution results in pathology. In: Honolulu, Hawaii: 25th International Society of Magnetic Resonance in Medicine. 1815.

Di X, Azeez A, Li X, Haque E, Biswal BB. 2018. Disrupted focal white matter integrity in autism spectrum disorder: a voxel-based meta-analysis of diffusion tensor imaging studies. Prog Neuropsychopharmacol Biol Psychiatry. 82:242–248.

Duerden EG, Mak-Fan KM, Taylor MJ, Roberts SW. 2012. Regional differences in grey and white matter in children and adults with autism spectrum disorders: an activation likelihood estimate (ALE) meta-analysis. Autism Res. 5: 49–66.

Gibbard CR, Ren J, Seunarine KK, Clayden JD, Skuse DH, Clark CA. 2013. White matter microstructure correlates with autism trait severity in a combined clinical-control sample of high-functioning adults. Neuroimage Clin. 3:106–114.

IBM Corp. 2016. IBM SPSS Statistics for Windows. Version 24.0. Armonk, NY: IBM Corp.

Im WY, Ha JH, Kim EJ, Cheon KA, Cho J, Song DH. 2018. Impaired white matter integrity and social cognition in high-function autism: diffusion tensor imaging study. Psychiatry Investig. 15:292–299.

Jeurissen B, Leemans A, Tournier JD, Jones DK, Sijbers J. 2013. Investigating the prevalence of complex fiber configurations in white matter tissue with diffusion magnetic resonance imaging. Hum Brain Mapp. 34:2747–2766.

Koldewyn K, Yendiki A, Weigelt S, Gweon H, Julian J, Richardson H, Malloy C, Saxe R, Fischl B, Kanwisher N. 2014. Differences in the right inferior longitudinal fasciculus but no general disruption of white matter tracts in children with autism spectrum disorder. Proc Natl Acad Sci USA. 111: 1981–1986.

Kumar A, Sundaram SK, Sivaswamy L, Behen ME, Makki MI, Ager J, Janisse J, Chugani HT, Chugani DC. 2010. Alterations in frontal lobe tracts and corpus callosum in young children with autism spectrum disorder. Cereb Cortex. 20: 2103–2113.

Lazar M, Miles LM, Babb JS, Donaldson JB. 2014. Axonal deficits in young adults with High Functioning Autism and their impact on processing speed. Neuroimage Clin. 4:417–425.

Lord C, Rutter M, DiLavore P, Risi S, Gotham K, Bishop S, Luyster R, Guthrie W. 2012. Autism Diagnostic Observation Schedule, Second Edition: ADOS-2. In. Los Angeles: Western Psychological Service.

McGrath J, Johnson K, O'Hanlon E, Garavan H, Gallagher L, Leemans A. 2013. White matter and visuospatial processing in autism: a constrained spherical deconvolution tractography study. Autism Res. 6:307–319.

Poustka L, Jennen-Steinmetz C, Henze R, Vomstein K, Haffner J, Sieltjes B. 2012. Fronto-temporal disconnectivity and symptom severity in children with autism spectrum disorder. World J Biol Psychiatry. 13:269–280.

Power JD, Barnes KA, Snyder AZ, Schlaggar BL, Petersen SE. 2012. Spurious but systematic correlations in functional connectivity MRI networks arise from subject motion. Neuroimage. 59:2142–2154.

Qiu A, Adler M, Crocetti D, Miller MI, Mostofsky SH. 2010. Basal ganglia shapes predict social, communication, and motor dysfunctions in boys with autism spectrum disorder. J Am Acad Child Adolesc Psychiatry. 49:539–551. 551.e531-534.

Raffelt D, Dhollander T, Tournier JD, Tabbara R, Smith RE, Pierre E, Connelly A. 2017. Bias field correction and intensity normalisation for quantitative analysis of apparent fiber density. In: Honolulu, Hawaii, United States: 25th International Society of Magnetic Resonance in Medicine. 3541.

Raffelt DA, Smith RE, Ridgway GR, Tournier JD, Vaughan DN, Rose S, Henderson R, Connelly A. 2015. Connectivity-based

fixel enhancement: whole-brain statistical analysis of diffusion MRI measures in the presence of crossing fibres. Neuroimage. 117:40–55.

Raffelt D, Tournier JD, Crozier S, Connelly A, Salvado O. 2012. Reorientation of fiber orientation distributions using apodized point spread functions. Magn Reson Med. 67:844–855.

Raffelt D, Tournier JD, Fripp J, Crozier S, Connelly A, Salvado O. 2011. Symmetric diffeomorphic registration of fibre orientation distributions. Neuroimage. 56:1171–1180.

Raffelt D, Tournier JD, Rose S, Ridgway GR, Henderson R, Crozier S, Salvado O, Connelly A. 2012. Apparent Fibre Density: a novel measure for the analysis of diffusion-weighted magnetic resonance images. Neuroimage. 59:3976–3994.

Raffelt DA, Tournier JD, Smith RE, Vaughan DN, Jackson G, Ridgway GR, Connelly A. 2017. Investigating white matter fibre density and morphology using fixel-based analysis. Neuroimage. 144:58–73.

Smith SM, Nichols TE. 2009. Threshold-free cluster enhancement: addressing problems of smoothing, threshold dependence and localisation in cluster inference. Neuroimage. 44:83–98.

Smith RE, Tournier JD, Calamante F, Connelly A. 2013. SIFT: spherical-deconvolution informed filtering of tractograms. Neuroimage. 67:298–312.

Solders SK, Carper RA, Müller RA. 2017. White matter compromise in autism? Differentiating motion confounds from true differences in diffusion tensor imaging. Autism Res. 10:1606–1620.

Tournier JD, Calamante F, Connelly A. 2007. Robust determination of the fibre orientation distribution in diffusion MRI: non-negativity constrained super-resolved spherical deconvolution. Neuroimage. 35:1459–1472.

Tournier JD, Calamante F, Connelly A. 2013. Determination of the appropriate b value and number of gradient directions for high-angular-resolution diffusion-weighted imaging. NMR Biomed. 26:1775–1786.

Travers BG, Adluru N, Ennis C, Tromp do PM, Destiche D, Doran S, Bigler ED, Lange N, Lainhart JE, Alexander AL. 2012. Diffusion tensor imaging in autism spectrum disorder: a review. Autism Res. 5:289–313.

Tustison NJ, Avants BB, Cook PA, Zheng Y, Egan A, Yushkevich PA, Gee JC. 2010. N4ITK: improved N3 bias correction. IEEE Trans Med Imaging. 29:1310–1320.

Wechsler D. 2011. Wechsler Abbreviated Scale of Intelligence, Second Edition (WASI-II). San Antonio, TX: NCS Pearson.

Yendiki A, Koldewyn K, Kakunoori S, Kanwisher N, Fischl B. 2014. Spurious group differences due to head motion in a diffusion MRI study. Neuroimage. 88:79–90.

Zikopoulos B, Barbas H. 2010. Changes in prefrontal axons may disrupt the network in autism. J Neurosci. 30:14595–14609.